ANALYSIS OF WIDE SPACED REINFORCED CONCRETE MASONRY SHEAR WALLS USING EXPLICIT FINITE ELEMENT METHOD

W. HAIDER* AND M. DHANASEKAR**

* Connell Hatch, 4740, Australia ** Central Queensland University, 4702, Australia

ABSTRACT

An explicit finite element modelling method for the analysis of shear walls of varying aspect ratios and vertical load levels is reported briefly. The program provides stable results until the crack pattern becomes excessive. This paper presents some results of the analysis of wide spaced reinforced concrete masonry shear walls containing door and window openings that are typical of low rise apartment buildings. Effect of variability of material properties on the behaviour of the walls is presented. The effect of opening sizes was also examined and some practical conclusions are drawn with reference to the simplified design provisions in AS3700.

INTRODUCTION

Masonry shear walls are generally modelled using static perturbation finite element modelling techniques based on implicit methods. Such finite element analyses of masonry walls in general, although have provided much insight, are regarded as too cumbersome and inefficient in terms of the time taken for the analysis. These conventional implicit techniques require solution of equilibrium equations containing the full stiffness matrix of the structure; as such they are very time consuming – typically tens of hours in high-performing workstations. Furthermore, as the masonry cracks the stiffness matrix tend to become ill-conditioned posing a convergence problem requiring attention to mesh pathology problems. In the absence of a reliable energy release criterion as part of the constitutive models, the solutions obtained based on homogenised macro modelling of masonry elements reported in the literature at best could only be regarded as providing indicative trends of the behaviour of masonry shear walls.

A computationally efficient explicit finite element modelling technique that is capable of simulating highly nonlinear events never requires a fully assembled system stiffness matrix; rather it solves for the internal variables using the theory of dynamic wave propagation in solids. Although the explicit technique is more suitable for high dynamic events such as impact, quasi-static load tests could also be simulated if due care is taken to minimise the kinetic energy due to rapid cracking/ load shedding. As iterations are not performed, much smaller increments of the applied load are required for the explicit technique to provide acceptable results. Converged solutions obtained from this technique are based on satisfaction of the global energy equilibrium equations; as such it is suitable where the global structural behaviour, such as the deformation and failure characteristics, is of prime importance. The explicit central difference time integration rule is used to satisfy the dynamic equilibrium equations shown in equation (1).

$$M\ddot{u} + U - W = 0 \qquad (1)$$

where u is the displacement vector; the global consistent mass matrix M , the internal energy U and external work done W. ABAQUS/Explicit generally requires 10,000 to 1,000,000

increments to achieve converged solutions, but the computational cost per increment is generally relatively small. For accuracy, the time increment is kept quite small. Maximum time increment used by the explicit solver related to the stability limit of the structure globally is calculated from the natural frequency corresponding mode shapes of a dynamic system. By artificially increasing the step time the velocities and the kinetic energy are minimised and hence stable and converged solution are achieved.

In this paper, analysis results of one of the WSRM prescriptive designs in AS3700 (2001) suitable for small buildings in the Australian regions of wind categories N4, C2 and earthquake categories H1, H2, H3 have been presented. This wall was modelled and analysed using the explicit FE model developed for the analysis of wide spaced reinforced masonry shear walls (WSRM) as a part of a PhD thesis (Haider (2007)). Vertical grouted reinforced cores and the bond beams were modelled using the REBAR option and the damaged plasticity concrete material model available in ABAQUS (2005). For unreinforced masonry sections of the wall, a user material subroutine (VUMAT) described in Haider (2007) was used to link the masonry material model developed by Lourenco (1996).

VARIABILITY IN MASONRY PROPERTIES

A standard normal distribution curve is commonly used for accounting for variation of data for many engineering applications. It is hypothysed that by adopting three standard deviations from the mean values and an inherent coefficient of variation (cov) equal to 20%, all types of masonry (clay block masonry, concrete block masonry, and calcium silicate masonry) could be accounted for. Average, maximum and minimum values of masonry material parameters for the walls obtained based on the above hypothesis are presented in Table 1.

$$\text{Max/Min Value} = \text{Mean} \pm 3\times(\text{cov}\times \textit{Mean}) \tag{2}$$

Table 1: Range of masonry material parameters

Parameter	Description	Units	Average Masonry (Mean)	Stronger Masonry (+3SD)	Weaker Masonry (-3SD)
f_{tx}	Tensile strength parallel to bed joints	MPa	0.60	0.96	0.24
G_{fx}	Fracture energy parallel to bed joints	N-mm/mm^2	1.0	1.6	0.4
f_{ty}	Tensile strength normal to bed joints	MPa	0.35	0.42	0.28
G_{fy}	Fracture energy normal to bed joints	N-mm/mm^2	0.5	0.8	0.2
f_{cx}	Comp. strength parallel to bed joints	MPa	3.0	4.8	1.2
G_{fcx}	Energy for compression failure parallel to bed joints	N-mm/mm^2	0.302	0.483	0.121
f_{cy}	Comp. strength normal to bed joints	MPa	10	28	7.2
G_{fcy}	Energy for compression failure normal to bed joints	N-mm/mm^2	4.35	6.96	1.74

Average values presented in Table 1 were collected from Literature (Page (1982), Dhanasekar (1985), Lourenco (1996)). Highest (stronger masonry) and lowest (weaker masonry) values of masonry material parameters were measured from equation (2). Using the means, the highest and the lowest values of masonry material parameters provided in Table 1, and the WSRM wall with varying door and window openings was analysed using the explicit FE model and the results are discussed in this paper.

MASONRY WALL FOR WIND CATEGORY N4, C2

A prescriptive design provided in AS3700 (2001) for a masonry shear wall suitable for small buildings in the Australian regions of wind category N4, C2 and earthquake category H1, H2, H3 is presented in Figure 1. Details of the wind categories for housing and the earthquake categories for the Australian regions can be found in AS4055 (2006) and AS1170.4 (1993) respectively. This design prescription is provided in Figure 12.8(B) of AS3700 (2001). This wall contains a maximum 1.8m wide opening for a door and a maximum 3m wide opening for a window within its length. Vertical reinforcement has been prescribed at the ends of openings and at a maximum spacing of 1.2m for the WSRM section of the wall. 16mm diameter bars (as shown in Figure 1) for the vertical grouted cores and 16mm and 12mm diameter bars for the bond beams are prescribed in this design.

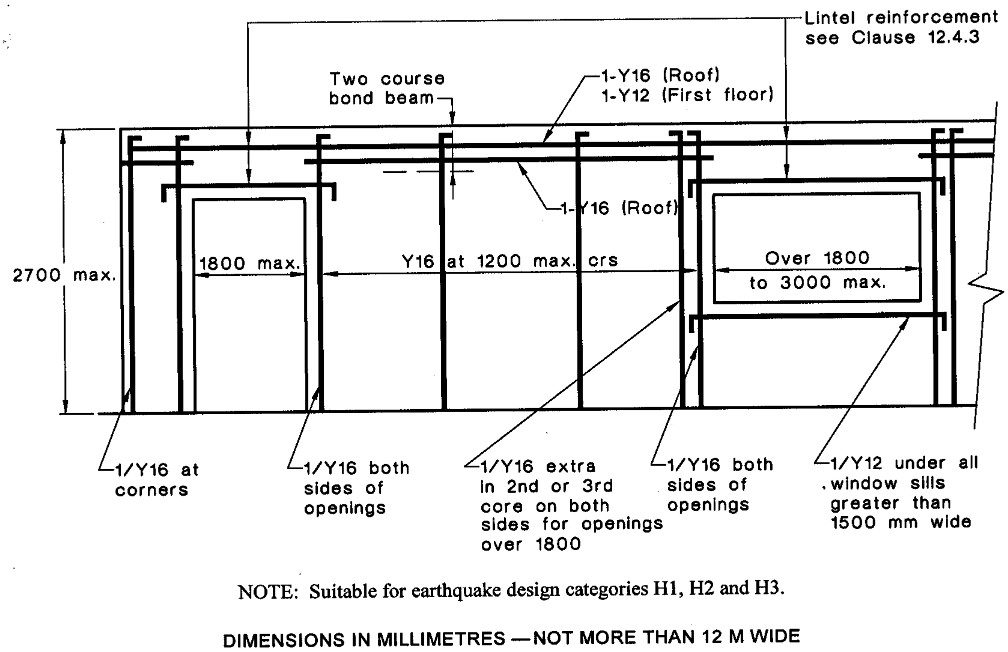

Figure 1: Simplified design prescribed in AS3700 (2001) for a 190mm thick masonry wall

AS3700 (2001) provides tables for racking load for small buildings containing these walls for different wind categories. The ultimate racking force for the wall shown in Figure 1 was read from chart K1 (j) of AS3700 (2001). Ultimate racking force resisted by the gable end of the 16m wide single or upper storey building with 30^{o} roof slope was 142kN and for the sub floor of a single storey maximum 1m above ground (high-set building) was 216kN. Based on the code provisions (AS3700 (2001)), the maximum racking load carried by the wall shown in Figure 1 would be equal to 71kN for single or upper storey building and 108kN when it forms part of an elevated single storey building maximum 1m above ground high-set building. These prescribed maximum loads were divided by the capacity reduction factor (0.75 as per clause 4.4 of AS3700 (2001)) to enable comparison with the FE predicted capacity. Therefore, modified values would be 95kN and 144kN respectively for single storey and high-set building shear walls.

FE ANALYSES OF A WALL WITH PRESCRIPTIVE DESIGN

A medium density mesh shown in Figure 2 was generated and used for the analysis of the 11m long wall. This wall is termed as Wall#1 here for convenience. The input data used for the wall shown in Figure 2 are as follows: area of each 16mm diameter reinforcement bar was $200mm^2$; thickness of the hollow masonry was 90mm (45mm face shell thickness) for 190mm hollow masonry blocks; thickness of the grouted cores was 190mm; and the thickness of the bond beam and the base slab was 190mm and 1000mm respectively. The width and height of the reduced integration plane stress elements (CPS4R) used for unreinforced masonry panels was 300mm and 180mm respectively. No vertical load was imposed since the ultimate capacity of the wall without the effect of the vertical load would provide the worst-case scenario. The bond beam and the vertical grouted cores were modelled as per the vertical and the horizontal reinforcement shown in Figure1. Only the elastic parameters (Young's modulus and Poisson's ratio) were defined for the bond beams, however complete compression hardening and tension stiffening data were provided to the FE model for the grout of the vertical reinforced grouted cores. The average masonry material parameters and stress–strain data for the reinforcement bars and compression hardening and tension stiffening data for the grout were provided to the FE model. Plots for the principal logarithmic strains and the principal stresses are presented in Figure 3(a) and 3(b) respectively.

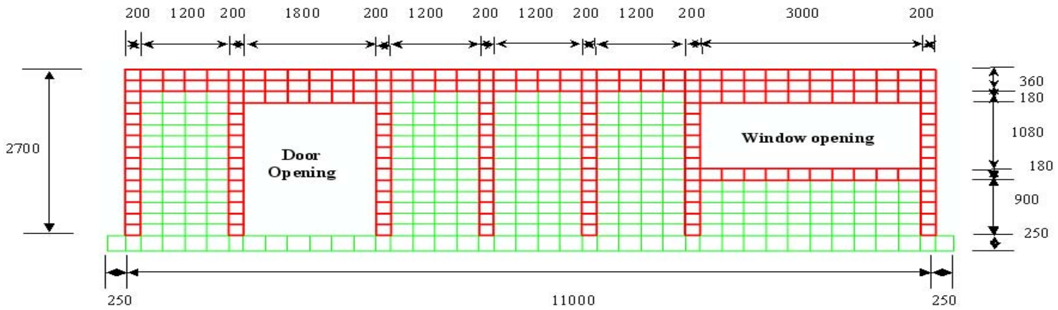

Figure 2: Mesh used for the analysis of wall #1

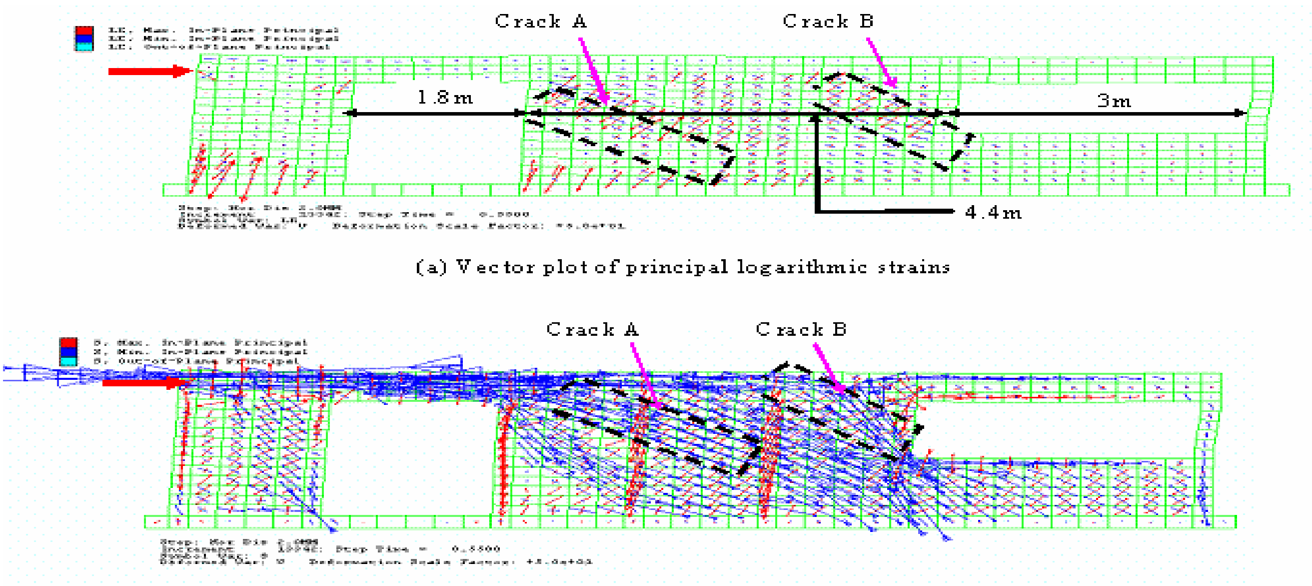

(a) Vector plot of principal logarithmic strains

(b) Vector plot of principal stresses

Figure 3: Principal strains and principal stresses for wall #1 (forward loading)

It can be seen from Figure 3 that the applied horizontal load concentrated mainly at the WSRM section between the two openings. Other sections appear to be resisting only a minor proportion of the horizontal load. Some heel tension was observed, however, the failure of the wall appears to be due to the diagonal failure of the middle WSRM section. Since the bond beams were modelled as elastic mediums, no failure occurred. Higher magnitudes of the logarithmic strain vectors along two separate diagonals (see Figure 3(a)) show the occurrence of two major cracks (crack A and crack B). Significant reduction in the magnitude of the principal stresses in the corresponding regions (see Figure 3(b)) confirmed the occurrence of the diagonal cracks.

Stress concentration in the path of the load flow at the corners of the openings was noticed, which is a typical engineering mechanics fundamental. It is important to note that the magnitude of the principal stresses in the WSRM section on the left side of the door opening and in the WSRM section below the window opening were quite low. This indicates that most of the applied horizontal load was resisted by the WSRM section between the two openings.

Displacement controlled horizontal load was applied in the reverse direction at the opposite end of the bond beam (right hand side of the window opening) at the top of the wall. Plots of principal logarithmic strains and principal stresses for the reverse direction loading can be found in Haider (2007). However, the load-displacement response of the wall obtained from the FE model for the forward and reverse loadings using average masonry material parameters is presented in Figure 4. No significant softening was predicted. Figure 4 shows that, under forward loading, the wall that was modelled as per the design prescription provided by AS3700 (2001) reached its ultimate load capacity of 350kN at approximately 2.5mm of horizontal displacement. Under the reverse loading, the same wall reached its ultimate load capacity of 275kN at approximately 1.8mm of horizontal displacement.

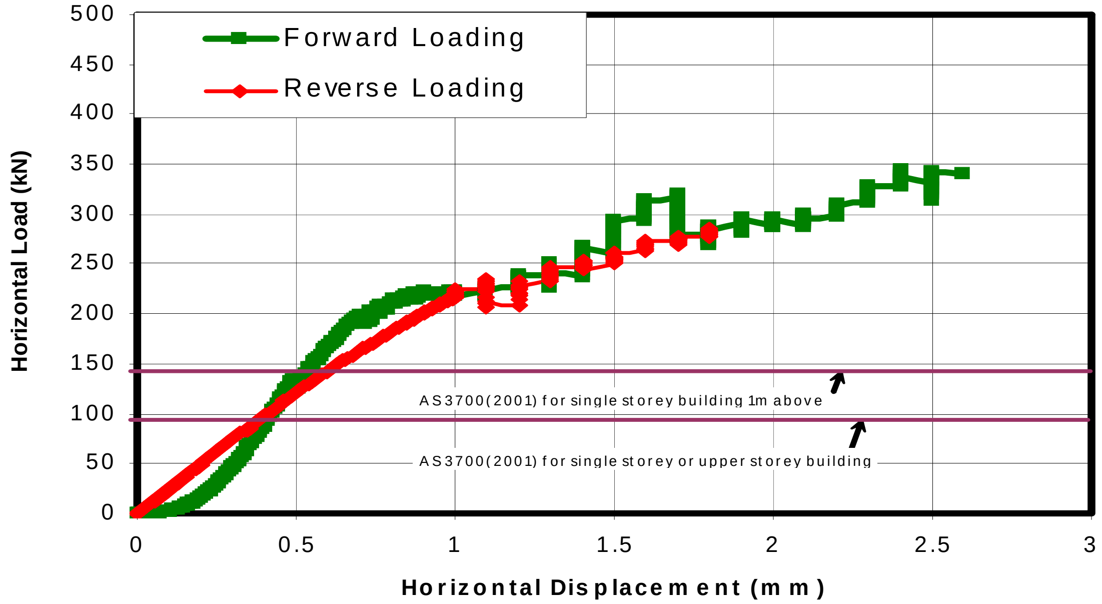

Figure 4: Load-displacement curve of wall #1 (Average Masonry)

The ultimate load predicted by the FE model for the forward loading and reverse loading was respectively 2.4 and 1.9 times the shear capacity value of 144kN prescribed by AS3700 (2001) for the high-set building shear walls. For the single storey and upper storey buildings, the ultimate load capacity predicted by the FE model was 3.7 and 2.9 times of the shear capacity value of 95kN prescribed by AS3700 (2001). Differences in the loading capacity for the forward and reverse loadings were due to the different width of the WSRM sections at the

two ends of the wall. For forward loading, the 1.6m wide WSRM end panel transferred the load to the middle WSRM section whereas for the reverse loading, only a 0.2m wide vertical grouted core was available to transfer the load.

Effect of Material Variability

Using average, stronger and weaker masonry material parameters provided in Table 1, the wall was analysed by applying the loading in the forward and reverse directions and the load-displacement curves are shown in Figures 5(a) and 5(b) respectively.

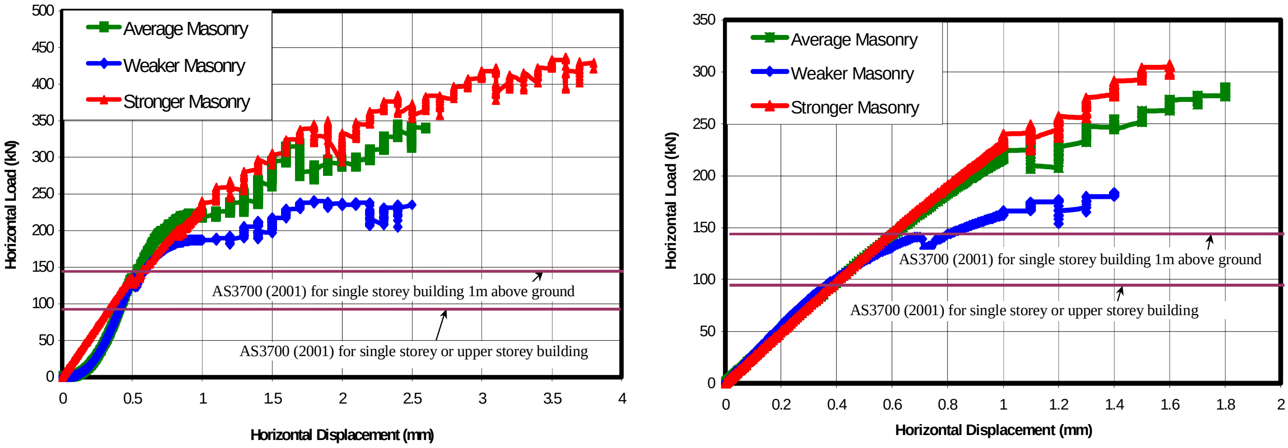

Figure 5: Load-displacement curve of the shear wall

From Figure 5(a), it is evident that, for walls irrespective of their materials of construction (clay block masonry or concrete block masonry or calcium silicate masonry), its actual shear capacity is more than its shear capacity value prescribed in AS3700 (2001). The load-displacement response of wall #1 in the reverse direction using average, stronger and weaker masonry is provided in Figure 5(b). From Figure 5(b), it is evident that, for the wall loaded in the reverse direction, the shear capacity predicted by the FE model is higher than the shear capacity values prescribed by AS3700 (2001). Predicted shear capacity value of the wall in the reverse direction is smaller than those in the forward direction, however, the reverse direction shear capacity values are slightly bigger than the AS3700 (2001) prescribed values.

Based on the FE analysis, it appears that the prescribed shear capacity values for WSRM walls for small buildings are sensible for the weaker masonry and a little conservative for stronger masonry. It would be ideal to include an engineering procedure for the design and analysis of such walls in AS3700 (2001) which will account for the material variability.

WALL WITH RELATIVELY LARGE OPENINGS

AS3700 (2001) prescriptions (Figure 1) do not allow for increase in the width of opening. The effect of the width of the opening to the shear capacity of the prescriptive wall (figure 1) was further studied by increasing the width of the door opening from 1.8m to 3.2m and keeping all other parameters the same. The mesh generated for the modified wall (termed as wall#2 here) design is shown in Figure 6. No vertical load was applied and the horizontal displacement was applied in the forward and reverse directions in multi steps using average masonry material parameters. The FE analysis was performed as described before and the response was interpreted.

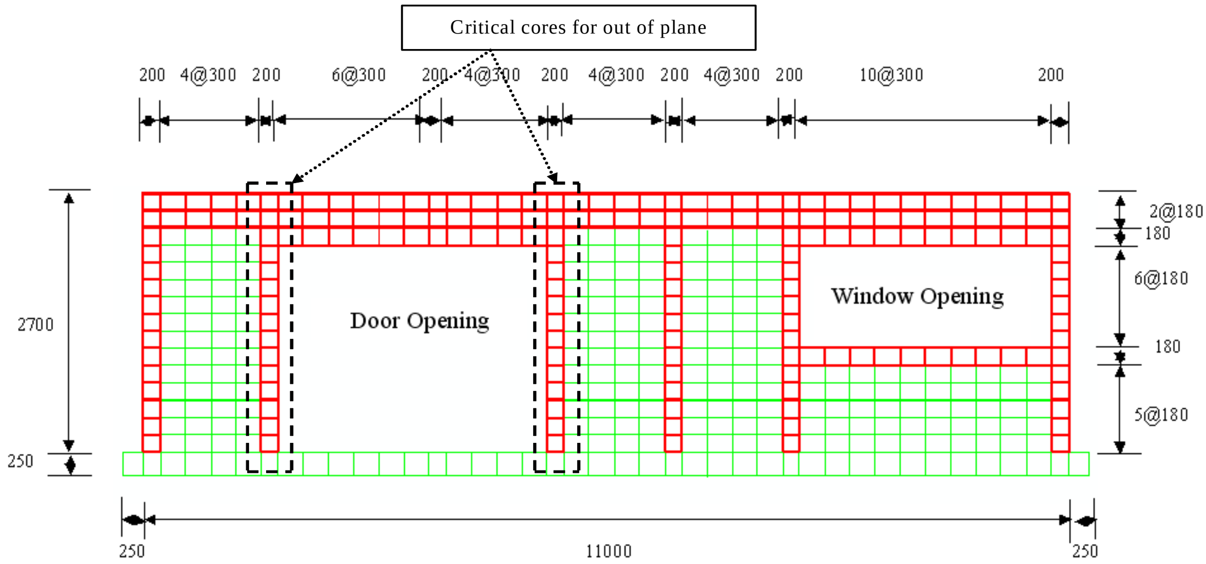

Figure 6: Mesh used for the analysis of wall #2

Principal logarithmic strains and the principal stresses are shown in Figures 7(a) and (b).

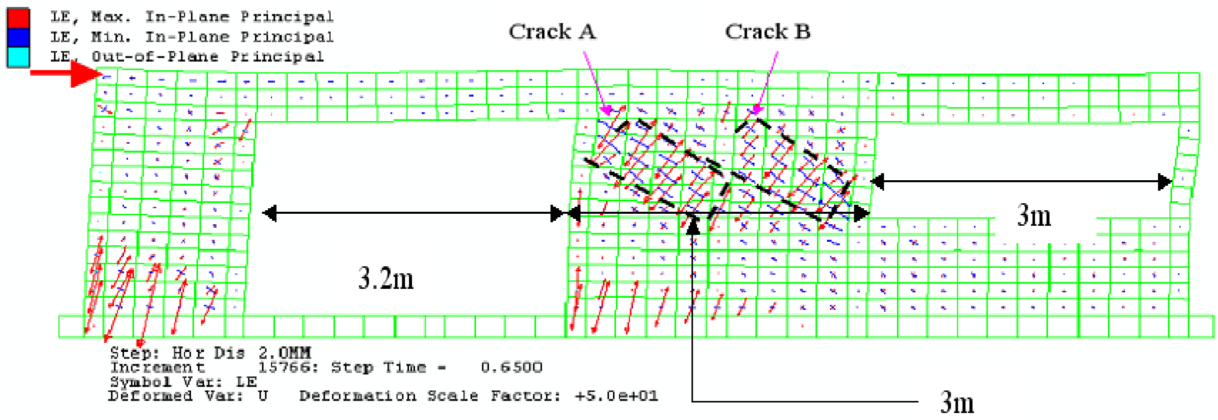

(a) Vector plot of principal logarithmic strains

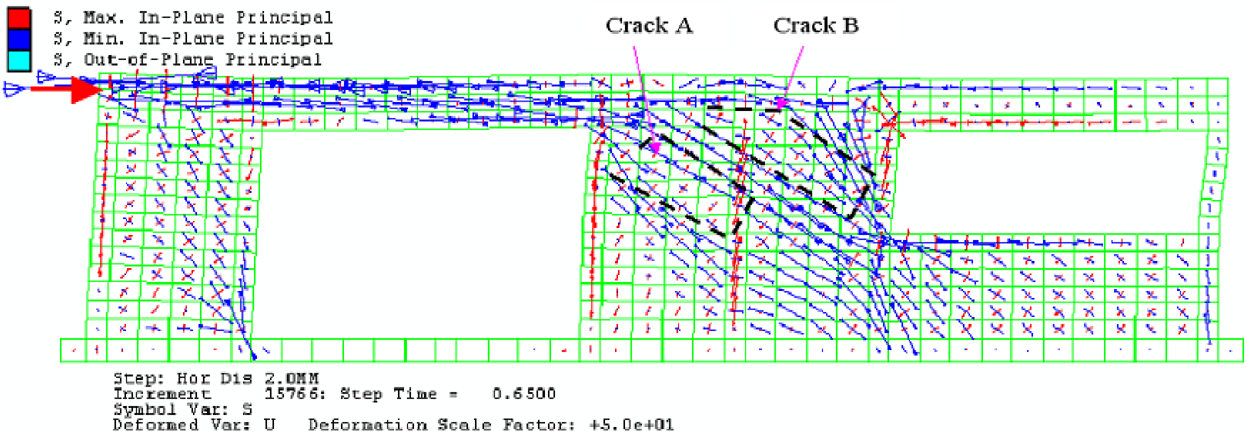

(b) Vector plot of principal stresses

Figure 7: Principal strains and principal stresses for wall #2 (forward loading)

The width of the door opening for this wall (wall #2) was set equal to 3.2m, which resulted in the reduction in the width of the middle WSRM section from 4.4m to 3m. In spite of such a significant increase in the width of the door opening (from 1.8m to 3.2m or 78% increase) and the corresponding reduction in the width of masonry between the openings, the load flow remained continuous similar to wall #1. The higher magnitude of principal strain vectors and the lower magnitude of principal stress vectors at two locations in the middle WSRM section of the wall indicated occurrence of two cracks (A and B). The distance between the two cracks decreased due to the reduced width of the middle WSRM section. Some heel tension was also noticed in this wall; however, the ultimate failure appears to be due to the diagonal failure of the WSRM section between the two openings. Displacement controlled horizontal load was applied in the reverse direction at the opposite end of the bond beam (right hand side of the window opening) at the top of this wall. Cracking pattern of wall #2 was also affected by the width of the end WSRM section. Most of the applied load was resisted by the middle WSRM section.

The load-displacement curves of wall #2 obtained from the FE model under forward and reverse loadings using average masonry material parameters are presented in Figure 8. No significant softening was noticed for this wall similar to wall #1. Figure 8 shows that the ultimate shear capacity of wall #2 under forward and reverse loading was approximately equal to 250kN and 175kN respectively. Both of these values are 100kN less than that of the corresponding values for wall #1. In other words, due to the increase in the width of the door opening and the corresponding reduction in the width of the WSRM panel between the two openings, the ultimate load capacity of this wall under the forward and reverse loading was reduced by 29% and 37% respectively. However, shear capacity of this wall (wall #2) under forward and reverse loading was still 42% and 18% higher than the modified prescribed shear capacity of 144kN in AS3700 (2001) for high-set building shear walls.

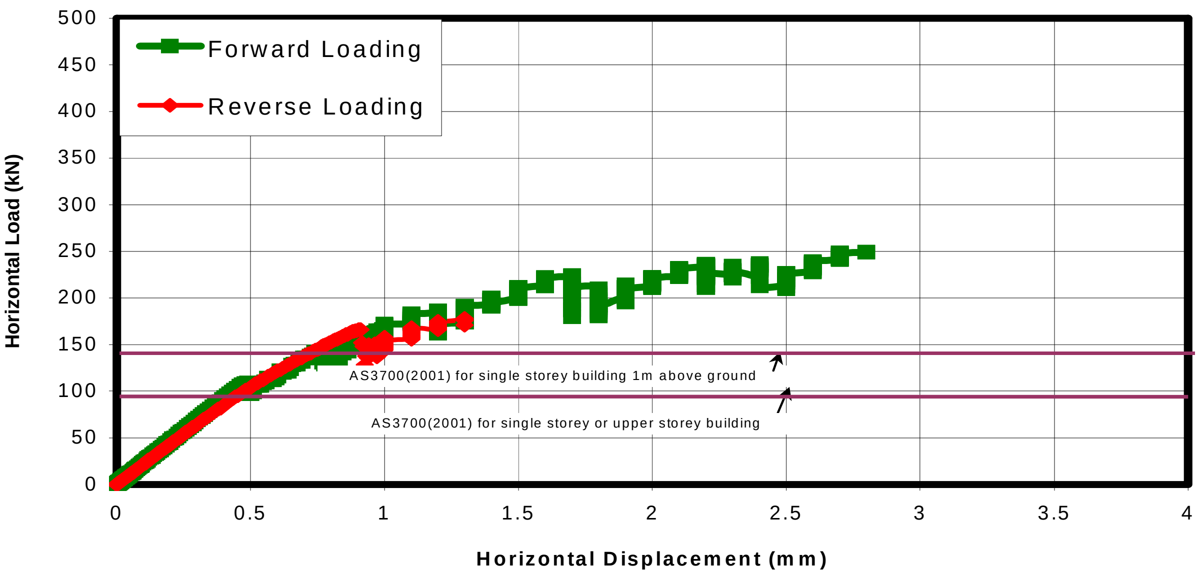

Figure 8: Load-displacement response of wall #2 (Average Masonry Properties)

It appears that the prescriptive design of the masonry wall that restricts the width of the door opening could also be adequate for 3.2m wide door opening if masonry with average material parameters is adopted in the construction. Relaxing the provisions of the simplified designs for small buildings in AS3700 (2001) is potentially possible and could allow for more design innovations and make masonry more attractive to designers

Effect of Material Variability

Similar to wall #1, wall #2 was also analysed using stronger and weaker masonry material parameters provided in Table 1, and the load-displacement curves for the forward and reverse directions are presented in Figures 9(a) and 9(b) respectively.

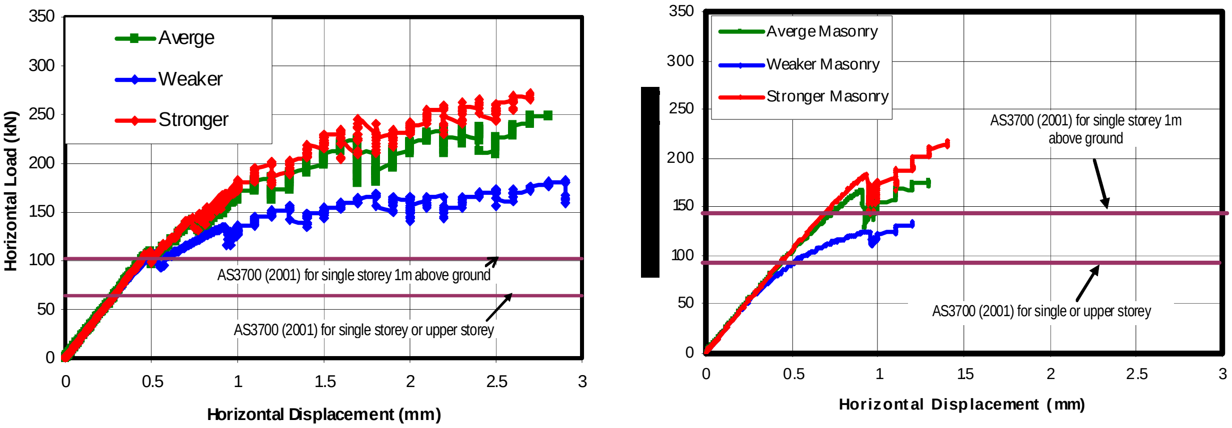

(a) Forward Loading (b) Reverse Loading

Figure 9: Load-displacement response of wall #2

Figure 9 (a) shows that the predicted shear capacity of wall #2 in the forward direction is 90%, 74%, and 21% higher than the AS3700 (2001) prescribed value of the shear capacity for wall #1 when it is constructed from stronger, average and weaker masonry respectively for a single storey building 1 m above the ground level. It appears that the limit on the width of door opening for the WSRM walls for small buildings could be increased.

DISCUSSIONS

The load-displacement curves of walls #1 and #2 under forward loading and reverse loading using weaker masonry are presented in Figure 10(a) and Figure 10(b) respectively. For both walls (#1 and #2) design details were kept the same, and only the width of the door opening was varied.

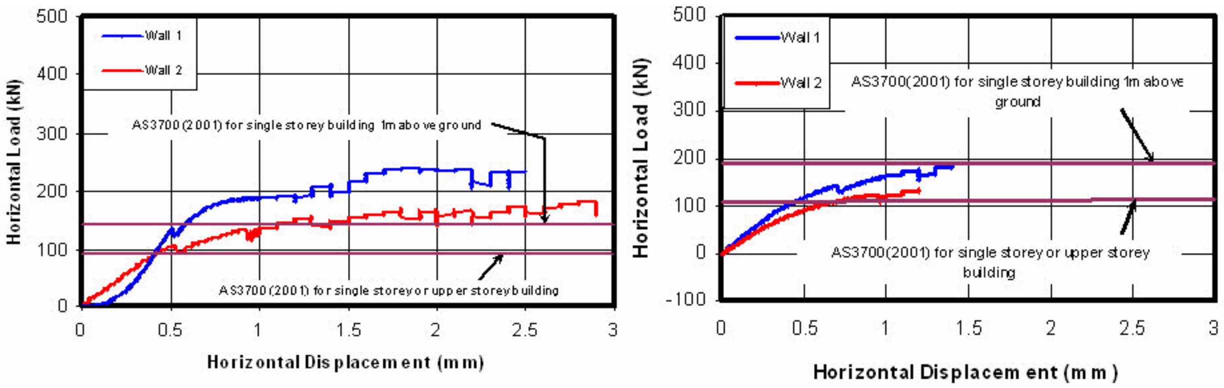

(a) Forward Loading – Non Critical (b) Reverse Loading – Critical

Figure 10: Load Displacement response of walls #1 and #2

Figure 10(a) shows that, using weaker masonry, the predicted shear capacity of walls #1 and #2 in the forward loading direction are 72% and 25% respectively higher than the prescribed

values for a single storey building 1 m above the ground.Figure 10(b) shows that, using weaker masonry, the predicted shear capacity of wall #1 in the forward direction is 25% higher than the prescribed values for a single storey building 1 m above the ground, whereas for wall #2, the predicted shear capacity is about 3% less than the prescribed value. Therefore the code of practice could not recommend construction of highest masonry homes with increased opening size in the N4/C2 wind zones. However increased opening size still appears sensible for single or double storey buildings (refer to the curve in red relative to the lower most line in Figure 10(b).

SUMMARY

The FE model developed for WSRM walls without major openings has provided sensible predictions of the load flow, the stress and strain distributions and the modes of failure of WSRM walls of 11m length with 3m wide openings. The load-displacement responses for the elastic and the strain hardening regimes have been obtained. It appears that the limit on the width of door opening for the WSRM walls for a small building could be increased if sufficiently large reinforced masonry section is provided on the path of load flow or masonry with stronger or at least average material parameters is adopted. More research is recommended to comprehensively investigate the appropriateness of the provisions of the design code for effective design of the WSRM walls.

ACKNOWLEDGEMENT

The project was financed by the ARC SPIRT Grant C00107223. The support and encouragement of the industry partner investigator Alan Pearson, Executive Director, Concrete Masonry Association of Australia and Professor Adrian Page, University of Newcastle are thankfully acknowledged.

REFERENCES

ABAQUS (2005). "*Theory Manual*", Hibbit, Karlson & Sorenson, Inc

AS1170.4 (1993). "*Australian Standards - Earthquake loads*" Standards Australia International.

AS3700 (2001). "*Australian Standards for Masonry Structures*" Standards Australia International.

AS4055 (2006). "*Australian Standards - Wind Loads for Housing*" Standards Australia International.

Dhanasekar, M. (1985), "The performance of brick masonry subjected to inplane loading", PhD Thesis, University of Newcastle, Australia.

Haider, W. (2007. "*Inplane Response of Wide Spaced Reinforced Masonry Shear Walls*" PhD Thesis, Central Queensland University, Australia.

Lourenco, P. B. (1996). "*Computational strategies for masonry structures" PhD* thesis, Delft University, Netherlands.

Page, A. W. (1982), "An experimental investigation of the biaxial strength of brick masonry" 6th International brick masonry conference, Rome, Italy, pp. 3-15.